Taylor & Francis
Taylor & Francis Group

BRIEF REPORT

Check for updates

Rab17 mediates intermixing of phagocytosed apoptotic cells with recycling endosomes

Charles Yin, Dean Argintaru, and Bryan Heit [ID]

Department of Microbiology and Immunology and the Centre for Human Immunology, The University of Western Ontario, London, Ontario, Canada

ABSTRACT

Efferocytosis—the phagocytic removal of apoptotic cells—is required for preventing the presentation of apoptotic cell-derived antigens. This process is regulated by Rab17-dependent sorting of efferocytosed cargos from the phagolysosome to recycling endosomes. In this study we demonstrate that Rab17 is rapidly recruited to efferosomes, followed by migration of the efferosome to the cell center where it intermixes with lysosomes and undergoes Rab17-dependent vesiculation. These efferosome-derived vesicles then traffic in a Rab17-dependent manner to the cell periphery, where they transfer cargo to recycling endosomes. Combined, our observations support a model wherein efferosomes migrate to the cell center to acquire degradative enzymes, followed by peripheral migration to prevent further phagolysosome maturation and to enable cargo transfer to recycling endosomes.

Introduction

In multicellular organisms the uptake of external materials through phagocytosis fulfills 2 functions: host defense and the clearance of apoptotic cells and debris.[1,2] Professional phagocytes such as macrophages or dendritic cells internalize and destroy pathogens[3] and present antigens to initiate adaptive immune responses.[1,4] Phagocytes also engage in efferocytosis—the phagocytosis of apoptotic materials,[1,5-7] but whereas pathogen phagocytosis results in immune activation and antigen presentation, efferocytosis is anti-inflammatory and does not elicit antigen-specific immunity.[8-10] Differential processing of antigens following phagocytosis versus efferocytosis is essential in maintaining immune silence, with defects in this process associated with inflammatory and autoimmune diseases including rheumatoid arthritis, and atherosclerosis.[7,11,12]

Phagocytosis is an actin-dependent process regulated by Rho family GTPases.[6,13] Following recognition of a target by phagocytic or efferocytic receptors (reviewed in refs. 8 and 14, Rac1 and Cdc42 mediate target internalization into a phagosome or efferosome,[6] which then mature through a shared maturation pathway regulated by the sequential acquisition of the GTPases Rab5 and Rab7.[15,16] Active Rab7 mediates fusion with lysosomes,[17]

resulting phagolysosome formation wherein cargo degradation and generation of antigen peptides occurs.[1,18] Thereafter, phagolysosomes evolve into a major histocompatibility complex II (MHC II) loading compartment, forming immunogenic MHC II-peptide complexes,[18] a process not observed with efferosomes.[9] The migration and fusion of the maturing phagosome with parts of the endolysosomal system is central to phagosome maturation and the processing of antigens,[1,2] and is driven by the dynein-dependent migration of nascent phagosomes from the cell periphery to the perinuclear area where phagosome-lysosome fusion occurs.[19] The recruitment of dynein is dependent on Rab7 and its effector RILP, with lysosomes lacking either Rab7 or RILP exhibiting defects in perinuclear trafficking, lysosomal fusion, acidification and cargo degradation.[17,20]

We have previously shown that Rab17 is selectively retained on the surface of efferosomes and functions to prevent the formation of the MHC II loading compartment.[21] Rab17 is a small GTPase, first identified in epithelial cells,[22,23] that has been implicated in the regulation of transcytosis,[24,25] dendrite formation in hippocampal neurons,[26] and melanosome exocytosis.[27]

Rab17 plays a key role as a regulator of basolateral to apical transport in polarized cells for cargos such as immunoglobulin A. Furthermore, it co-localizes with the recycling endosome markers transferrin receptor (TfR) and FcLR chimeric receptor,[28] suggesting that it mediates trafficking of material through the recycling endosome network. Although the regulation of Rab17 remains only partially characterized, it is established that Rab17 can be activated by the guanine exchange factor Rabex5,[29] and mediates vesicular fusion through syntaxin 2.[22] As Rab17 is an important regulator of the migration and fusion of intracellular vesicles and functions to direct efferocytic cargo away from the MHC II loading compartment, we investigated the mechanism by which Rab17 regulates the transfer of efferosome cargos to recycling endosomes and away from the canonical phagolysosome maturation pathway.

Results

Rab17 sorts materials on maturing efferosomes

We previously demonstrated that Rab17 is rapidly recruited to efferosomes, where it mediates the transfer of degraded apoptotic cell materials from the efferosome to recycling endosomes.[21] Here, we sought to elucidate the mechanism by which Rab17 mediates the transfer of materials from efferosomes to recycling endosomes. Firstly, the distribution of Rab17 relative to recycling endosomes (demarcated by transferrin receptor, TfR) and plasma-membrane derived vesicles (demarcated by PM-RFP) was assessed in resting macrophages. PM-RFP was excluded from Rab17$^+$ vesicles (Fig. 1A, C); more interestingly, while all but a minute portion of Rab17$^+$ vesicles were positive for TfR, there was a significant portion of TfR$^+$ vesicles which lacked Rab17 (Fig. 1B, C). Therefore, in resting macrophages, Rab17 demarcates a subset of the recycling endosome system and is not significantly recruited to plasma membraned-derived vesicles such as endosomes.

Next, live cell microscopy was used to quantify Rab17 dynamics during efferocytosis, using large (5 μm) apoptotic cell mimics to provide high spatial resolution (Fig. 1D, Movie S1). These mimics were internalized into a PM-RFP demarcated compartment which was positive for GFP-Rab17. A few minutes following closure, the efferosome vesiculated through the fission of Rab17$^+$ vesicles, depleting approximately 60% of the Rab17 initially recruited to the efferosome (Fig 1D, Table 1). Interestingly, the fissioning vesicles were devoid of PM-RFP, suggesting that materials were being selectively sorted during efferosome vesiculation. The efferosome remained weakly positive for Rab17 following vesiculation, with the occasional Rab17$^+$ vesicle interacting with the efferosome during this stage (data not shown).

Fission and fusion of efferosome-derived vesicles

Our initial results used indigestible apoptotic cell mimics, thus preventing us from relating Rab17 dynamics to the processing of the efferosomal cargo. To address this limitation, Rab17 dynamics were quantified on efferosomes containing labeled apoptotic Jurkat cells in macrophages expressing mCherry-Rab17 and PM-GFP. Macrophages engulfed apoptotic bodies, not intact cells (Table 1, Fig. 2A), with the level of Rab17 retained on efferosomes and the size of the efferosomes remaining constant during the early stages of maturation (Table 1, Fig. 2B). Despite some photobleaching, it was apparent that newly formed efferosomes migrated toward the cell center where they then vesiculated into multiple efferosome-derived vesicles (EDVs, Fig. 2B–C). Interestingly, the intensity of PM-GFP staining on EDVs was variable, consistent with the sorting observed during the vesiculation of non-digestible efferosome mimics (Fig. 2B). By tracking the fluorescent signal of the apoptotic bodies we were able to track EDVs for prolonged periods of time, revealing that newly vesiculated EDVs migrated toward the cell periphery, and once at the cell periphery, ceased moving (Fig. 2B, C). During this migration most EDVs underwent further vesiculation, as well as fusion with other EDVs and with Rab17$^+$ recycling endosomes that were otherwise devoid of apoptotic bodies (Fig. 2B–D, Table 1), consistent with our previous study demonstrating cargo transfer from efferosomes to TfR-positive recycling endosomes.[21] Both the inward movement of the nascent efferosome, and the subsequent outward movement of the EDVs were highly linear, but became non-directional once EDVs reached the cell periphery (Fig. 2E–G).

Rab17 is required for edv migration

The inward migration of the newly formed efferosome is required for efficient fusion with lysosomes and cargo degradation,[17,30] and indeed, our previous work demonstrated efferosome-lysosome fusion concordant with Rab17 recruitment to the efferosome.[21] In contrast, the subsequent peripheral migration of phagocytosed cargo is, to our knowledge, previously unreported. To determine if Rab17 was required for peripheral efferosome migration, we expressed dominant-negative (DN) or wildtype (WT) GFP-Rab17 in macrophages and quantified the intracellular localization of efferosomes, using DN-Rab17 at a modest expression level to prevent the inhibition of efferocytosis observed when Rab17 siRNA is used.[21] As expected, a significant fraction of efferosomes were located in the periphery of cells expressing WT-Rab17, whereas efferosomes remained in the central area of cells expressing DN-Rab17 (Fig. 3A–B). Efferosomes in DN-Rab17 expressing cells underwent limited fission (Fig. 3C–D,
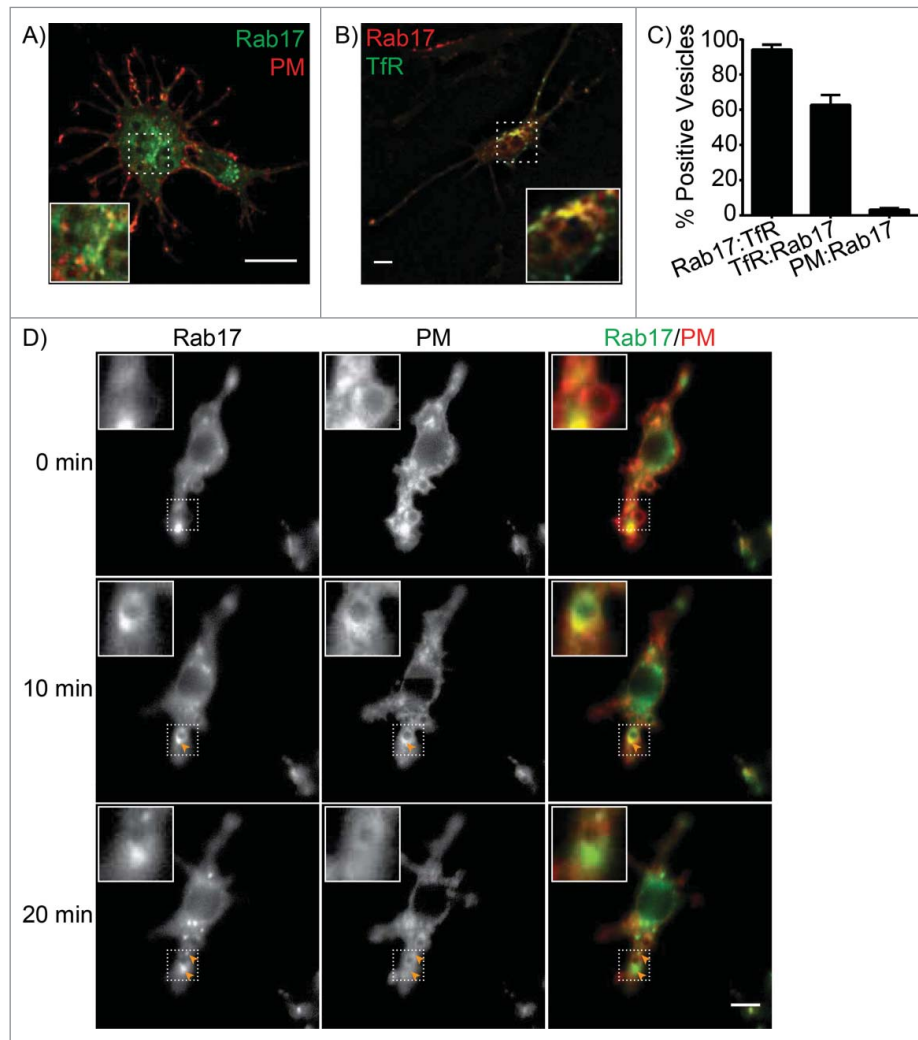
Figure 1. Rab17 Dynamics on Efferosome Mimics. (A-B) Co-localization of GFP- or mCherry-Rab17 with plasma-membrane (PM-RFP) derived vesicles (A) or with transferrin receptor (TfR-GFP) positive vesicles (B) in resting macrophages. (C) Percent of Rab17$^+$ vesicles co-staining with TfR (Rab17:TfR), TfR$^+$ vesicles co-staining with Rab17 (TfR:Rab17) and PM-derived vesicles co-staining with Rab17 (PM:Rab17) in resting macrophages. (D) Dynamics of GFP-Rab17 and the plasma membrane marker PM-RFP on efferosomes containing non-digestible apoptotic cell mimics. Orange arrows indicate Rab17+ vesicles fissioning from the efferosome. Images are representative of (A-B) and quantifies (C) 47 images captured over 4 independent experiments, or is representative of 12 time-lapse videos captured over 5 independent experiments (D). Data is presented as mean ± SEM. Scale bars are 5 μm (A-B) or 10 μm (D).

Table 1. Efferosome fission and fusion characteristics.

Efferosome Characteristics	Mimics	Apoptotic Cells
Diameter at Closure	5.20 ± 1.4 μm	2.87 ± 0.13 μm
Diameter at Vesiculation	4.97 ± 2.6 μm	2.74 ± 0.11 μm
Time to Vesiculation	7.25 ± 3.72 min	22.40 ± 3.78 min
Number of EDVs/Efferosome	1.25 ± 0.45	4.05 ± 0.58
Vesiculation Time	3.25 ± 1.29 s	*
Size of EDVs	1.08 ± 0.29 μm	**
Time from Vesiculation to First Fusion	n.o.	10.77 ± 2.23 min
DN-Rab17 Efferosome Characteristics		
Time to Vesiculation	—	64.1 ± 10.3 min
Number of EDVs/Efferosomes	—	0.79 ± 0.51
Size of EDVs	—	2.28 ± 0.46 μm

*Vesiculation time was shorter than the time between video frames (120 s)
**Many vesicles were sub-resolution in size and could not be measured
n.o. Not Observed

Table 1), but fused normally with LAMP1-demarkated lysosomes (Fig. 3E, G). Consistent with our previous work, expression of DN-Rab17 significantly impaired the transfer of efferosome cargos from EDVs to transferrin-positive recycling endosomes (Fig. 3F, G).

Discussion

In this study we have identified a Rab17-dependent vesiculation, fusion and trafficking process that is required for the transfer of degraded apoptotic cells from the efferosome to the recycling endosome. Our data are consistent with a model in which newly formed efferosomes traffic to the central region of macrophages to
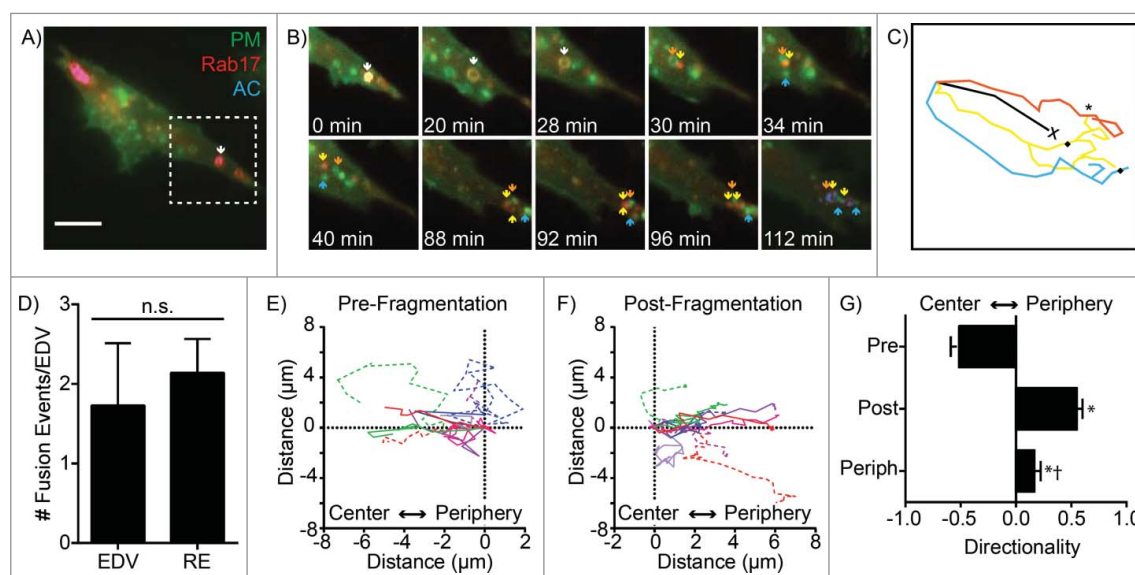
Figure 2. Fission, Fusion and Movement of Rab17-Positive Efferosomes. Efferosome and Rab17 dynamics were quantified using live cell microscopy of efferocytosed fluorescently-labeled apoptotic bodies by macrophages expressing mCherry-Rab17 and PM-GFP. (A) Fluorescent image of a macrophage immediately following engulfment of an apoptotic body (arrow/AC), scale bar is 5 μm. (B) Time-lapse micrograph of the insert from panel A. The intact efferosome is tracked by the white arrow, colored arrows track individual EDVs. The staining of the apoptotic body is shown only for the first and final frames, to emphasize the differential sorting of Rab17 and PM-GFP into EDVs. (C) Track of efferosome and EDVs from panel B. 'X' indicates the efferosome starting position, asterisk indicates fusion between 2 EDVs, and diamonds indicate sites of fusion with Rab17-positive recycling endosomes. (D) Number of fusion events between EDVs, and between EDV and recycling endosomes (RE). (E) Representative motion tracks of 10 pre-fission efferosomes, measured relative to a vector between the cell barycentre and the site of efferosome formation. (F) Representative motion tracks of a single post-fission vesicle derived from each efferosome in panel E, measured relative to a vector between the cell barycentre and the efferosome fission point. (G) Directionality of efferosome movement pre-fission (Pre), Post-fission (Post), and once the EDVs reach the periphery (Periph). Data is representative of (A-C, E, F), or quantifies (D, G) 124 efferosomes imaged over 3 independent experiments. * = p < 0.05 comparted to Pre, $\dagger$ = p < 0.05 compared with Post, n.s. = p > 0.05, Students t-test (D) or ANOVA with Tukey correction (G).

fuse with lysosomes, but then avoid subsequent maturation into a MHC II loading compartment through trafficking to the cell periphery where their cargo is transferred to recycling endosomes[31-33] This sorting is mediated by Rab17, which drives the fragmentation, peripheral migration, and cargo transfer from EDVs to recycling endosomes, thereby delivering degraded apoptotic cells to the recycling pathway and preventing development of the phagolysosome into a MHC II loading compartment.

The observation that efferosomes undergo an initial migration to the cell center is consistent with the maturation of bacteria-containing phagosomes.[17,30,34] In phagocytosis, active Rab7 recruits the effector RILP, which associates with the dynactin complex and drives perinuclear migration of phagosomes, where they undergo fusion with lysosomes to form phagolysosomes.[17,35] Consistent with this model, we previously demonstrated that efferosomes acquire Rab7 a few minutes after closure,[21] and in this study demonstrate Rab17-independent efferosome migration to the cell center and Rab17-independent fusion with lysosomes.

Therefore, the initial inward migration of efferosomes is likely a product of Rab7 activity on the efferosome and results in the acquisition of lysosomal enzymes for cargo degradation. In contrast, while phagolysosomes remain in the perinuclear region,[17,35] efferosomes undergo a distinct secondary outward migration, during which time they fuse with other EDVs and with TfR-demarcated recycling endosomes. This may represent a process whereby Rab17 moves degraded material from late in the endocytic/phagocytic pathway to the recycling endosome.[21] While the initial inward migration and lysosomal fusion were Rab17 independent, the later outward migration of EDV and fusion with EDVs and recycling endosomes were dependent on active Rab17. As Rab17 is a key regulator of the transcytosis of macromolecules through the recycling endosome compartment,[24,25,28] it is tempting to hypothesize that the outward migration of EDVs to the cell periphery and cargo transfer to recycling endosomes may result in the exocytosis of degraded apoptotic bodies, although we have not yet observed direct evidence in support of this hypothesis.
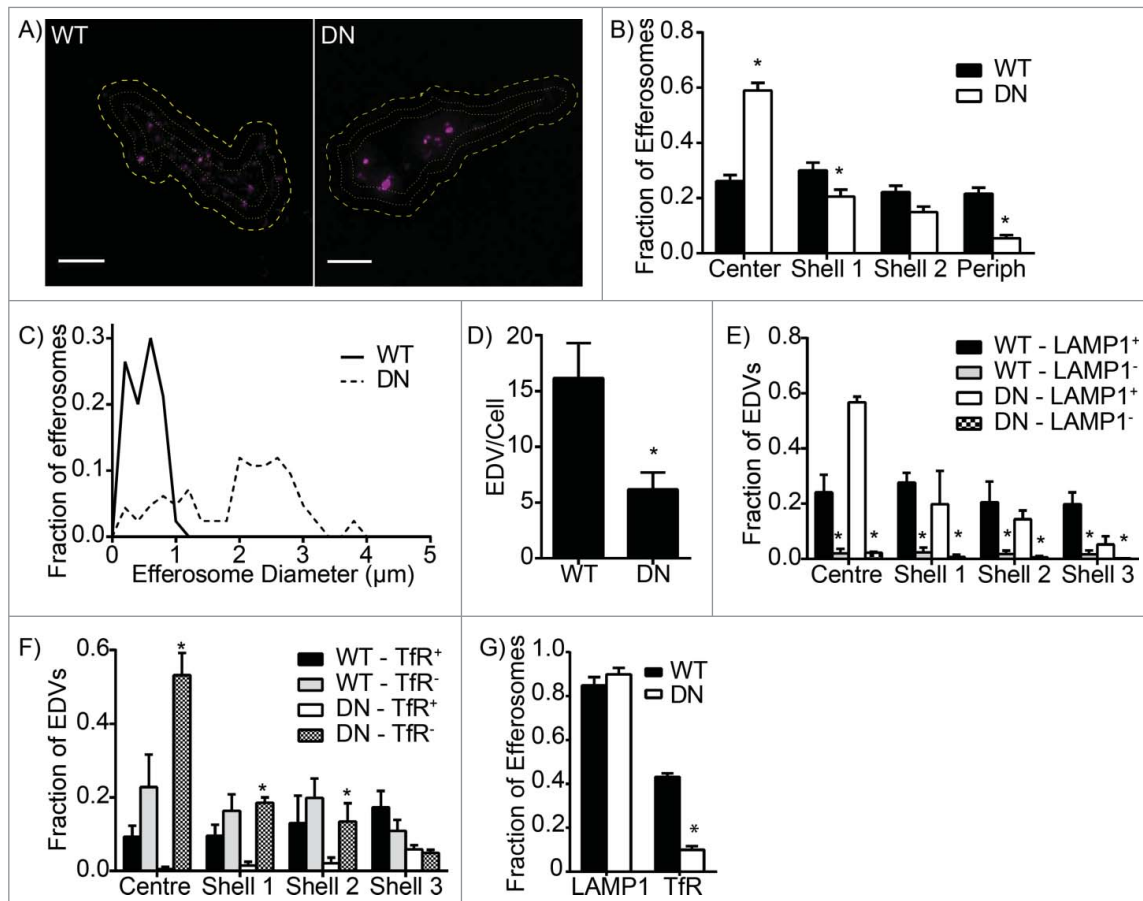
Figure 3. Peripheral Migration of EDVs and Cargo Transfer to Recycling Endosomes Requires Rab17. Localization of fluorescently labeled, Jurkat cell-derived EDVs in macrophages expressing wild-type (WT) or dominant-negative (DN) GFP-Rab17, and either the lysosomal marker LAMP1-mCherry or the recycling endosome marker TfR-mCherry, was quantified 90-minutes post-efferocytosis. (A) Representative images of EDV location in cells expressing WT- or DN-Rab17. Large dashed line indicates the cell periphery; fine dotted lines indicate "shells" positioned at 1 μm increments inwards from the cell periphery. (B) Quantification of the fraction of EDVs observed in each "shell" of cells expressing wild-type or dominant-negative Rab17. (C-D) Diameter (C) and number (D) of EDVs in macrophages expressing WT- and DN-Rab17. (E) Effect of WT- vs. DN-Rab17 on the distribution of EDVs colocalizing with (LAMP1$^+$) or lacking (LAMP1$^-$) the lysosomal marker LAMP1. (F) Effect of WT- vs. DN-Rab17 on the distribution of EDVs colocalizing with (TfR$^+$) or lacking (TfR$^-$) the recycling endosome marker TfR. (G) Total colocalizaiton of efferosomes with LAMP1 and TfR in cells expressing WT- or DN-Rab17. n = 33 (WT) or 28 (DN) cells, imaged over 3 independent experiments. * p < 0.05 compared with WT (B, G), LAMP$^+$ in the same group (E) or TfR$^+$ in the same group (F), 2-way ANOVA with Tukey correction, or Students t-test (D, G). Scale bars are 5 μm.

While our data are consistent with a model in which apoptotic cell-derived antigens are trafficked away from the lysosome/MHC II loading compartment to avoid presentation of self-antigens, this is unlikely to be the sole mechanism preventing presentation of self-antigens from efferosomes. Indeed, MHC II is rapidly turned over in cells, and requires TLR signaling to stabilize its expression and enable its delivery to the maturing phagosome.[32,33,36] TLR signaling is suppressed by efferocytosis, likely accounting for the lack of MHC II recruitment to efferosomes.[21,37] In addition, the lysosomes of macrophages polarized to the pro-efferocytic M2 phenotype acidify more strongly than lysosomes in macrophages polarized to non-efferocytic M1 phenotypes, indicating that efferocytic cargos will be highly processed by acid

hydrolases, perhaps to a degree where MHC II compatible peptides are not produced.[38] Finally, full activation of CD4+ T cells requires not only antigen presentation on MHC II, but also strong expression of co-stimulatory molecules such as CD80 and CD86. These molecules are weakly expressed on highly efferocytic M2 macrophages, and are upregulated following TLR stimulation, indicating that even if apoptotic cell derived antigen are loaded onto MHC II, the resulting presentation may be minimally immunogenic.[33,39] These and other pathways likely cooperate to limit the immunogenicity of efferocytosed apoptotic cells.

In summary, we have demonstrated that Rab17 mediates a previously uncharacterized vesicular fission and migration process required for the transfer of degraded

apoptotic bodies from a phagolysosome-like compartment to recycling endosomes. This process likely represents a mechanism whereby degraded apoptotic materials are recycled or expelled through exocytosis to avoid antigen presentation and the generation of autoimmunity.

Methods and materials

Materials

Transferrin receptor-GFP/mCherry (Tfn-GFP/mCherry), LAMP1-mCherry and plasma-membrane-GFP/mCherry (PM-GFP/mCherry) were gifts from Sergio Grinstein (Hospital for Sick Children, Toronto, Canada), wild-type and dominant-negative Rab17 constructs were described previously.[21] Jurkat T cells and DH5a *Escherichia coli* were gifts from Drs. Jimmy Dikeakos and John McCormick (University of Western Ontario). J774.2 macrophages were purchased from CedarLane (Mississauga, Canada). #1.5/18mm circular coverslips and 16% paraformaldehyde (PFA) were purchased from Electron Microscopy Supplies (Hatfield, Pennsylvania). Permafluor, T4 DNA ligase, FugeneHD and Phusion DNA polymerase were purchased from Thermo Scientific (Mississauga, Canada). Cell Proliferation Dye eFluor 670 was purchased from eBioscience (San Diego, CA). DMEM, RPMI and Fetal Bovine Serum (FBS) were purchased from Wisent (Saint-Jean-Baptiste, Canada). Silica beads were purchased from Bangs Laboratories (Fishers, Indiana). Phosphatidylserine and phosphatidylcholine were purchased from Avanti Polar Lipids (Alabaster, Alabama). All other chemicals were purchased from Canada BioShop (Mississauga, Canada). Matlab software was purchased from MathWorks (Natick, Massachusetts), Graphpad Prism statistical software was purchased from Graphpad (La Jolla, California) and FIJI Is Just ImageJ (FIJI) was downloaded from https://fiji.sc/.

J774.2 culture

J774.2 macrophages were maintained in adherent culture using T25 tissue culture flasks containing 5 ml DMEM + 10% FBS in a 37°C/5% CO_2 incubator. Cells were split at confluency by cell scraping and dilution into fresh media. For experiments, coverslips were placed into the wells of a 12-well plate and ~2.5×10^5 cells in culture medium placed into each well. Cells were transfected with 1.1 μg of DNA and 3.3 μl of FugeneHD as per manufactures instructions.

Apoptotic mimics

Mimics were prepared as described previously.[21,40] 0.4 mmol of a lipid mixture containing 80% phosphatidylcholine and 20% phosphatidylserine in chloroform were measured into a glass vial, 10 μl of 5 μm diameter silica beads added, the mixture vortexed and chloroform evaporated under nitrogen for 1 hr. The beads were then suspended in 1 ml of PBS (137 mM NaCl, 2.7 mM KCl, 10 mM Na_2HPO_4, 1.8 mM KH_2PO_4), washed $3\times$ in PBS using $4500\times$g/1 min centrifugations, suspended 100 μl of DMEM + 10% FBS and stored at 4°C until use.

Jurkat apoptosis model

Jurkat cells were maintained in suspension in T25 culture flasks containing 5 ml RPMI + 10% FBS. Cells were split every 3 d by diluting 1:10 into fresh media. 5 ml of Jurkat cell culture was pelleted using a 5 min/250$\times$g centrifugation and apoptosis induced by 4 hrs incubation at 37°C in serum-free RPMI + 1 μM staurosporine.[40,41] Cells were washed $3\times$ in PBS, labeled with 2 μl/ml Cell Proliferation Dye eFluor 670 for 5 min, washed $2\times$ with PBS and diluted in DMEM + 10% FBS to 1×10^6 cells/ml.

Efferocytosis assays

For live-cell experiments, coverslips were transferred to a Leiden chamber on the heated/CO_2 perfused stage of a Leica DMI6000B microscope equipped with a 100$\times$/1.40 NA objective, photometrics Evolve-512 delta EM-CCD camera, Chroma Sedat Quad filter set and the Leica Application Suite X software platform (Leica Microsystems, Concord, ON, Canada). The location of 5–10 transfected cells were stored using the mark-and-find feature, then 1 mL of the apoptotic Jurkat cell suspension or 1 ml of DMEM + 3 μl of mimics added. Cells were recorded using the GFP, RFP and far-red channels for 2 hours at 0.5 FPS.[40] For fixed cell imaging, 1 mL of apoptotic cells or 1 ml of DMEM + 3 μl of mimics were added to each well, the plate centrifuged at 200 $\times$ g for 1 min, and the plate incubated at 37°C/5% CO_2 for 60–90 min. Samples were rinsed once with PBS, fixed with 4% PFA in PBS for 20 min, rinsed with PBS and mounted on glass coverslips using Permafluor mounting media.[40] A minimum of 15 cells imaged on each coverslip. Images were exported as OME-formatted TIFFs for further analysis.

Efferosome mimics quantification

Quantification of mimic-containing efferosomes was performed using FIJI. Time to fragmentation was measured from the timepoint of complete efferosome closure to the fission of the first Rab17^{+} EDV, and the number of EDVs formed recorded. EDV diameter was quantified using the line measurement tool.

Colocalization analysis

Colocalization analysis was performed with FIJI. Non-vesicular staining was reduced using a 5-pixel rolling-ball subtraction, the image manually thresholded to remove cytosolic staining, and regions of interest (ROIs) created for individual EDVs using the analyze particles tool. Colocalization between markers was then quantified as the fraction of overlapping of ROI's between channels.

Efferosome fission, fusion and movement

Efferosomes were tracked in fluorescent images using FIJI. At the timepoint of efferosome closure an ROI was drawn around the cell using the freehand selection tool, and the x/y coordinates of the cell barycentre determined with the measure tool. The MTrack2 plugin was used to track the efferosome, EDVs, and any EDV-interacting Rab17$^+$ vesicles. Track positions were imported into Matlab, the timing and location of all fission and fusion events annotated, and the track divided into pre- vs. post-initial fission segments. Pre-fission tracks were translated such that all measurements were made relative to a vector linking efferosome closure site to the cell barycentre, and post-fission tracks translated such that all measurements were made relative to a vector linking the fission site to the cell barycentre. The directionality of movement of each track was then quantified as the ratio between the Euclidian distance covered by the vesicle from its start- to end-point vs. the total distance traveled.[42,43]

Efferosome positioning

Efferosome positioning was quantified using the method of Johnson et al.[20] A 90 min efferocytosis assay was performed using fluorescently labeled apoptotic Jurkat cells and J774.2 macrophages expressing wild-type or dominant-negative GFP-Rab17, co-transfected with LAMP1-mCherry or TfR-mCherry. Images were imported into FIJI and the cell boundary, as defined by the Rab17 staining, traced using the freehand tool. This ROI was then degraded inwards in 1 μm increments to create 3 shells of 1 μm thickness. The number of EDVs in each shell, EDV diameter (sub-resolution EDVs were recorded as 0.2 μm in diameter), and colocalization with LAMP or TfR was quantified in each image using the protocols described above.

Statistics

Graphapd Prism software was used for all statistical tests. Data are presented as mean $\pm$ SEM, with statistical significance set at p $\leq$ 0.05.

Abbreviations

EDV	Efferosome Derived Vesicle
MHC II	Major Histocompatability Complex II
PBS	Phosphate Buffered Saline
PFA	Paraformaldehyde
ROI	Region of Interest
TfR	Transferrin Receptor

Disclosure of potential conflicts of interest

No potential conflicts of interest were disclosed.

ORCID

Bryan Heit http://orcid.org/0000-0003-2392-468X

References

[1] Blander JM, Medzhitov R. On regulation of phagosome maturation and antigen presentation. Nat Immunol 2006; 7:1029-35; PMID:16985500; http://dx.doi.org/10.1038/ni1006-1029

[2] Kinchen JM, Ravichandran KS. Phagosome maturation: going through the acid test. Nat Rev Mol Cell Biol 2008; 9:781-95; PMID:18813294; http://dx.doi.org/10.1038/nrm2515

[3] Flannagan RS, Cosío G, Grinstein S. Antimicrobial mechanisms of phagocytes and bacterial evasion strategies. Nat Rev Microbiol 2009; 7:355-66; PMID:19369951; http://dx.doi.org/10.1038/nrmicro2128

[4] Kapsenberg ML, Teunissen MB, Stiekema FE, Keizer HG. Antigen-presenting cell function of dendritic cells and macrophages in proliferative T cell responses to soluble and particulate antigens. Eur J Immunol 1986; 16:345-50; PMID:3486127; http://dx.doi.org/10.1002/eji.1830160405

[5] Kojima Y, Volkmer J-P, McKenna K, Civelek M, Lusis AJ, Miller CL, Direnzo D, Nanda V, Ye J, Connolly AJ, et al. CD47-blocking antibodies restore phagocytosis and prevent atherosclerosis. Nature 2016; 536(7614):86-90

[6] Kinchen JM, Doukoumetzidis K, Almendinger J, Stergiou L, Tosello-Trampont A, Sifri CD, Hengartner MO, Ravichandran KS. A pathway for phagosome maturation during engulfment of apoptotic cells. Nat Cell Biol 2008; 10:556-66; PMID:18425118; http://dx.doi.org/10.1038/ncb1718

[7] Thorp E, Cui D, Schrijvers DM, Kuriakose G, Tabas I. Mertk receptor mutation reduces efferocytosis efficiency and promotes apoptotic cell accumulation and plaque

necrosis in atherosclerotic lesions of apoe−/− mice. Arterioscler Thromb Vasc Biol 2008; 28:1421-8; PMID:18451332; http://dx.doi.org/10.1161/ATVBAHA.108.167197

[8] Korns D, Frasch SC, Fernandez-Boyanapalli R, Henson PM, Bratton DL. Modulation of macrophage efferocytosis in inflammation. Front Immunol 2011; 2:1-10; PMID:22566792; http://dx.doi.org/10.3389/fimmu.2011.00057

[9] McGaha TL, Chen Y, Ravishankar B, Rooijen N Van, Karlsson MCI, Mcgaha TL, Chen Y, Ravishankar B, Rooijen N Van, Karlsson MCI. Marginal zone macrophages suppress innate and adaptive immunity to apoptotic cells in the spleen. Blood 2011; 117:5403-12; PMID:21444914; http://dx.doi.org/10.1182/blood-2010-11-320028

[10] Sotomayor EM, Borrello I, Rattis FM, Cuenca AG, Abrams J, Staveley-O'Carroll K, Levitsky HI. Cross-presentation of tumor antigens by bone marrow-derived antigen-presenting cells is the dominant mechanism in the induction of T-cell tolerance during B-cell lymphoma progression. Blood 2001; 98:1070-7; PMID:11493453; http://dx.doi.org/10.1182/blood.V98.4.1070

[11] Muñoz LE, Lauber K, Schiller M, Manfredi A a, Herrmann M. The role of defective clearance of apoptotic cells in systemic autoimmunity. Nat Rev Rheumatol 2010; 6:280-9; PMID:20431553; http://dx.doi.org/10.1038/nrrheum.2010.46

[12] Fonseca JE, Edwards JCW, Blades S, Goulding NJ. Macrophage subpopulations in rheumatoid synovium: Reduced CD163 expression in CD4+ T lymphocyte-rich microenvironments. Arthritis Rheum 2002; 46:1210-6; PMID:12115225; http://dx.doi.org/10.1002/art.10207

[13] Elliott MR, Ravichandran KS. The Dynamics of Apoptotic Cell Clearance. Dev Cell 2016; 38:147-60; PMID:27459067;http://dx.doi.org/10.1016/j.devcel.2016.06.029

[14] Freeman SA, Grinstein S. Phagocytosis: Receptors, signal integration, and the cytoskeleton. Immunol Rev 2014; 262:193-215; PMID:25319336; http://dx.doi.org/10.1111/imr.12212

[15] Roberts RL, Barbieri MA, Ullrich J, Stahl PD. Dynamics of Rab5 activation in endocytosis and phagocytosis. J Leukoc Biol 2000; 68:627-32; PMID:11073100

[16] Rupper A, Grove B, Cardelli J. Rab7 regulates phagosome maturation in Dictyostelium. J Cell Sci 2001; 114:2449-60; PMID:11559753

[17] Harrison RE, Bucci C, Vieira O V, Schroer TA, Grinstein S. Phagosomes fuse with late endosomes and/or lysosomes by extension of membrane protrusions along microtubules: role of Rab7 and RILP. Mol Cell Biol 2003; 23:6494-506; PMID:12944476; http://dx.doi.org/10.1128/MCB.23.18.6494-6506.2003

[18] Rocha N, Neefjes J. MHC class II molecules on the move for successful antigen presentation. EMBO J 2008; 27:1-5; PMID:18046453; http://dx.doi.org/10.1038/sj.emboj.7601945

[19] Rai A, Pathak D, Thakur S, Singh S, Dubey AK, Mallik R. Dynein clusters into lipid microdomains on phagosomes to drive rapid transport toward lysosomes. Cell 2016; 164:722-34; PMID:26853472; http://dx.doi.org/10.1016/j.cell.2015.12.054

[20] Johnson DE, Ostrowski P, Jaumouillé V, Grinstein S. The position of lysosomes within the cell determines their luminal pH. J Cell Biol 2016; 212:677-92; PMID:26975849; http://dx.doi.org/10.1083/jcb.201507112

[21] Yin C, Kim Y, Argintaru D, Heit B. Rab17 mediates differential antigen sorting following efferocytosis and phagocytosis. Cell Death Dis 2016; 7:e2529; PMID:28005073; http://dx.doi.org/10.1038/cddis.2016.431

[22] Striz AC, Tuma PL. The GTP-bound and sumoylated form of the RAB17 small molecular weight GTPase selectively binds syntaxin 2 in polarized hepatic WIF-B cells. J Biol Chem 2016; 291(18):9721-32; jbc.M116.723353; PMID:26957544

[23] Lütcke A, Jansson S, Parton RG, Chavrier P, Valencia A, Huber LA, Lehtonen E, Zerial M. Rab17, a novel small GTPase, is specific for epithelial cells and is induced during cell polarization. J Cell Biol 1993; 121:553-64; PMID:8486736; http://dx.doi.org/10.1083/jcb.121.3.553

[24] Hansen GH, Niels-Christiansen LL, Immerdal L, Hunziker W, Kenny AJ, Danielsen EM. Transcytosis of immunoglobulin A in the mouse enterocyte occurs through glycolipid raft- and Rab17-containing compartments. Gastroenterology 1999; 116:610-22; PMID:10029620; http://dx.doi.org/10.1016/S0016-5085(99)70183-6

[25] Hunziker W, Peters PJ. Rab17 localizes to recycling endosomes and regulates receptor-mediated transcytosis in epithelial cells. J Biol Chem 1998; 273:15734-41; PMID:9624171; http://dx.doi.org/10.1074/jbc.273.25.15734

[26] Mori Y, Matsui T, Furutani Y, Yoshihara Y, Fukuda M. Small GTPase Rab17 regulates dendritic morphogenesis and postsynaptic development of hippocampal neurons. J Biol Chem 2012; 287:8963-73; PMID:22291024; http://dx.doi.org/10.1074/jbc.M111.314385

[27] Beaumont KA, Hamilton NA, Moores MT, Brown DL, Ohbayashi N, Cairncross O, Cook AL, Smith AG, Misaki R, Fukuda M, et al. The Recycling Endosome Protein Rab17 Regulates Melanocytic Filopodia Formation and Melanosome Trafficking. Traffic 2011; 12:627-43; PMID:21291502; http://dx.doi.org/10.1111/j.1600-0854.2011.01172.x

[28] Zacchi P, Stenmark H, Parton RG, Orioli D, Lim F, Giner A, Mellman I, Zerial M, Murphy C. Rab17 regulates membrane trafficking through apical recycling endosomes in polarized epithelial cells. J Cell Biol 1998; 140:1039-53; PMID:9490718; http://dx.doi.org/10.1083/jcb.140.5.1039

[29] Mori Y, Matsui T, Fukuda M. Rabex-5 protein regulates dendritic localization of small GTPase Rab17 and neurite morphogenesis in hippocampal neurons. J Biol Chem 2013; 288:9835-47; PMID:23430262; http://dx.doi.org/10.1074/jbc.M112.427591

[30] Cantalupo G, Alifano P, Roberti V, Bruni CB, Bucci C. Rab-interacting lysosomal protein (RILP): The Rab7 effector required for transport to lysosomes. EMBO J 2001; 20:683-93; PMID:11179213; http://dx.doi.org/10.1093/emboj/20.4.683

[31] Saric A, Hipolito VEB, Kay JG, Canton J, Antonescu CN, Botelho RJ. mTOR controls lysosome tubulation and antigen presentation in macrophages and dendritic cells. Mol Biol Cell 2016; 27:321-33; PMID:26582390; http://dx.doi.org/10.1091/mbc.E15-05-0272

[32] ten Broeke T, Wubbolts R, Stoorvogel W. MHC class II antigen presentation by dendritic cells regulated through endosomal sorting. Cold Spring Harb Perspect Biol 2013; 5:a016873; PMID:24296169; http://dx.doi.org/10.1101/cshperspect.a016873

[33] Cho K-J, Walseng E, Ishido S, Roche PA. Ubiquitination by March-I prevents MHC class II recycling and promotes MHC class II turnover in antigen-presenting cells. Proc Natl Acad Sci U S A 2015; 112:10449-54; PMID:26240324; http://dx.doi.org/10.1073/pnas.1507981112

[34] Fairn GD, Grinstein S. How nascent phagosomes mature to become phagolysosomes. Trends Immunol 2012; 33 (8):397-405

[35] Cui Y, Zhao Q, Gao C, Ding Y, Zeng Y, Ueda T, Nakano A, Jiang L. Activation of the Rab7 GTPase by the MON1-CCZ1 complex is essential for PVC-to-vacuole trafficking and plant growth in Arabidopsis. Plant Cell 2014; 26:2080-97; PMID:24824487; http://dx.doi.org/10.1105/tpc.114.123141

[36] Walseng E, Furuta K, Bosch B, Weih KA, Matsuki Y, Bakke O, Ishido S, Roche PA. Ubiquitination regulates MHC class II-peptide complex retention and degradation in dendritic cells. Proc Natl Acad Sci U S A 2010; 107:20465-70; PMID:21059907; http://dx.doi.org/10.1073/pnas.1010990107

[37] Das A, Ganesh K, Khanna S, Sen CK, Roy S. Engulfment of Apoptotic Cells by Macrophages: A Role of Micro-RNA-21 in the Resolution of Wound Inflammation. J Immunol 2014; 192:1120-9; PMID:24391209; http://dx.doi.org/10.4049/jimmunol.1300613

[38] Canton J, Khezri R, Glogauer M, Grinstein S. Contrasting phagosome pH regulation and maturation in human M1 and M2 macrophages. Mol Biol Cell 2014; 25:3330-41; PMID:25165138; http://dx.doi.org/10.1091/mbc.E14-05-0967

[39] Dalli J, Serhan CN. Specific lipid mediator signatures of human phagocytes: microparticles stimulate macrophage efferocytosis and pro-resolving mediators. Blood 2012; 120:e60-72; PMID:22904297; http://dx.doi.org/10.1182/blood-2012-04-423525

[40] Evans AL, Blackburn JWD, Yin C, Heit B. Quantitative Efferocytosis Assays. Methods Mol Biol 2017; 1519:25-41; PMID:27815871

[41] Heit B, Yeung T, Grinstein S. Changes in mitochondrial surface charge mediate recruitment of signaling molecules during apoptosis. Am J Physiol Cell Physiol 2011; 300:C33-41; PMID:20926778; http://dx.doi.org/10.1152/ajpcell.00139.2010

[42] Heit B, Tavener S, Raharjo E, Kubes P. An intracellular signaling hierarchy determines direction of migration in opposing chemotactic gradients. J Cell Biol 2002; 159:91-102; PMID:12370241; http://dx.doi.org/10.1083/jcb.200202114

[43] Heit B, Kubes P. Measuring chemotaxis and chemokinesis: the under-agarose cell migration assay. Sci STKE 2003; 2003:PL5; PMID:12591998